Summary report for special agreement TAL-NAPC20210119-007

Cédric Jouanne

October 19, 2021

1 Introduction

This document presents results of criticality and shielding benchmarks calculated using five of the latest evaluation libraries made available in recent years : TENDL-17[1], TENDL-19[1], JEFF-3.3[2], JENDL-4-0 [3] and ENDF/B-VIII[4]. All the calculations are performed with the Monte Carlo codes TRIPOLI-4® [5].
TRIPOLI-4 is the fourth generation of the continuous-energy three-dimensional transport Monte Carlo code developed by the Service d'Études des Réacteurs et de Mathématiques Appliquées (SERMA) at CEA Saclay (FRANCE). TRIPOLI-4 is devoted to shielding, reactor physics with depletion, criticality safety and nuclear instrumentation for both fission and fusion systems. The code has been has been developed starting from the mid 90s in C++, with a few parts in C and Fortran. The latest release of TRIPOLI-4 is version 11, as of November 2018.

2 Criticality Benchmarks calculations

2.1 PMF1

This benchmark, named Jezebel, consists of a 6.3849cm sphere made of plutonium and gallium. Figure 1, Table 1 and Table 2 present results obtained with MCNP6 and TRIPOLI-4® using various libraries.

Code-Lib	MCNP6-B8	T4.11-B8	MCNP6-T17	T4.11-T17	T4.11-T19	T4.11-J33
k_{eff}	1.00069 (1)	0.99970 (2)	1.00114 (1)	1.00022 (2)	1.00008 (2)	0.99917 (2)

Table 1: PMF1 benchmark Jezebel : MCNP6 and TRIPOLI-4.11 k_{eff} calculations using ENDF/B-VIII, JEFF-3.3,TENDL-17 and TENDL-19 libraries

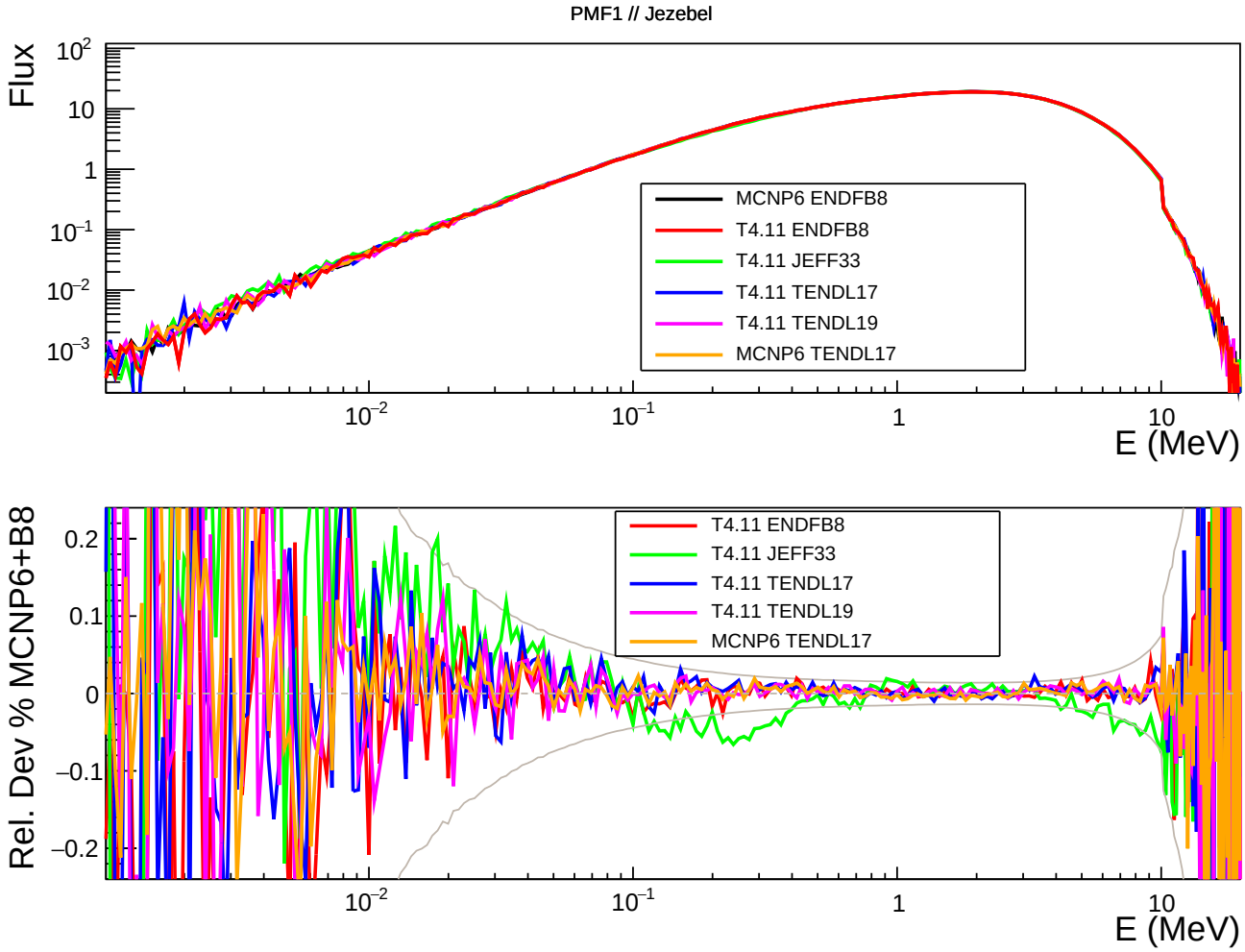

Figure 1: Results on neutron flux for PMF1 benchmark Jezebel. Upper part : neutron flux. Lower part : ratio to MCNP5.1.40 + TENDL-19.

Reaction	MCNP6-B8	T4.11-B8	MCNP6-T17	T4.11-T17	T4.11-T19	T4.11-J33
U233(n,f)	1.58270E-2	1.58450E-2	1.58415E-2	1.58723E-2	1.58615E-2	1.56160E-2
U235(n,f)	1.01071E-2	1.01177E-2	1.01162E-2	1.01359E-2	1.01291E-2	1.00344E-2
U238(n,f)	2.14418E-3	2.14443E-3	2.14591E-3	2.14839E-3	2.14836E-3	2.10801E-3
U238(n,2n)	1.33668E-4	1.33165E-4	1.33619E-4	1.34077E-4	1.33347E-4	1.26745E-4
U238(n,γ)	6.50377E-4	6.51674E-4	6.51092E-4	6.52773E-4	6.51926E-4	6.29016E-4
Np237(n,f)	9.87822E-3	9.88269E-3	9.80592E-3	9.82196E-3	9.82474E-3	9.87230E-3
Np237(n,2n)	2.37250E-5	2.35441E-5	2.32130E-5	2.33683E-5	2.31056E-5	2.24035E-5
Pu239(n,f)	1.44271E-2	1.44416E-2	1.44363E-2	1.44624E-2	1.44561E-2	1.44058E-2
Pu239(n,2n)	3.32137E-5	3.30910E-5	3.32489E-5	3.33114E-5	3.31885E-5	3.72303E-5
Am241(n,γ)	3.29154E-3	3.29784E-3	3.30838E-3	3.31844E-3	3.31120E-3	3.23121E-3
Al27(n,p)	2.99840E-5	2.99810E-5	3.05687E-5	3.05394E-5	3.12745E-5	2.91455E-5
Al27(n,α)	6.49445E-6	6.45679E-6	6.37745E-6	6.40948E-6	6.15754E-6	6.15884E-6
P31(n,p)	2.32644E-4	2.32869E-4	2.45370E-4	2.45476E-4	2.47425E-4	1.95025E-4
V51(n,γ)	2.31553E-5	2.31962E-5	2.78737E-5	2.80616E-5	2.44670E-5	2.31963E-5
Mn55(n,γ)	2.85681E-5	2.85008E-5	2.84936E-5	2.87063E-5	2.88547E-5	2.83478E-5
Fe56(n,p)	9.30413E-6	9.27075E-6	9.32194E-6	9.33366E-6	9.29856E-6	8.73268E-6
Cu63(n,2n)	1.06881E-6	1.05920E-6	1.06348E-6	1.08462E-6	1.01084E-6	1.03546E-6
Cu63(n,γ)	1.02003E-4	1.02523E-4	8.93228E-5	8.93768E-5	9.10547E-5	1.02266E-4
Nb93(n,γ)	2.77792E-4	2.78520E-4	2.62692E-4	2.63513E-4	2.59474E-4	2.77530E-4
Rh103(n,γ)	7.96079E-4	7.98336E-4	9.21768E-4	9.24196E-4	9.11845E-4	8.69664E-4
Ag107(n,γ)	1.06165E-3	1.06314E-3	8.17007E-4	8.19545E-4	6.36891E-4	6.36642E-4
Sb121(n,γ)	9.22161E-4	9.23194E-4	8.49434E-4	8.51717E-4	8.35895E-4	7.46028E-4
La139(n,γ)	6.25914E-5	6.25003E-5	6.06222E-5	6.07057E-5	5.92066E-5	6.24175E-5
Tm169(n,2n)	3.77961E-5	3.71501E-5	3.78379E-5	3.83855E-5	3.74649E-5	3.42093E-5
Tm169(n,γ)	1.07024E-3	1.07222E-3	8.58745E-4	8.62290E-4	8.47218E-4	8.55261E-4
Ir191(n,2n)	3.81573E-5	3.75249E-5	4.43713E-5	4.49883E-5	4.17126E-5	3.55718E-5
Ir191(n,γ)	1.57068E-3	1.57300E-3	1.99926E-3	2.00477E-3	2.02225E-3	1.56006E-3
Ir193(n,γ)	1.14892E-3	1.15056E-3	9.02697E-4	9.05793E-4	9.34700E-4	1.14149E-3
Au197(n,γ)	7.77068E-4	7.77839E-4	7.79998E-4	7.81925E-4	7.76679E-4	7.68206E-4
Bi209(n,γ)	2.24036E-5	2.24247E-5	1.97141E-5	1.97177E-5	1.95198E-5	1.72720E-5

Table 2: PMF1 benchmark Jezebel : MCNP6 and TRIPOLI-4.11 reaction rates calculations using ENDF/B-VIII, JEFF-3.3,TENDL-17 and TENDL-19 libraries

2.2 PMF2

This benchmark, named Jezebel-Pu40, consists of a 6.6595cm sphere made of plutonium and gallium. The concentration of Pu240 is much higher than in PMF1. Figure 2, Table 3 and Table 4 present results obtained with MCNP6 and TRIPOLI-4.11 using various libraries.

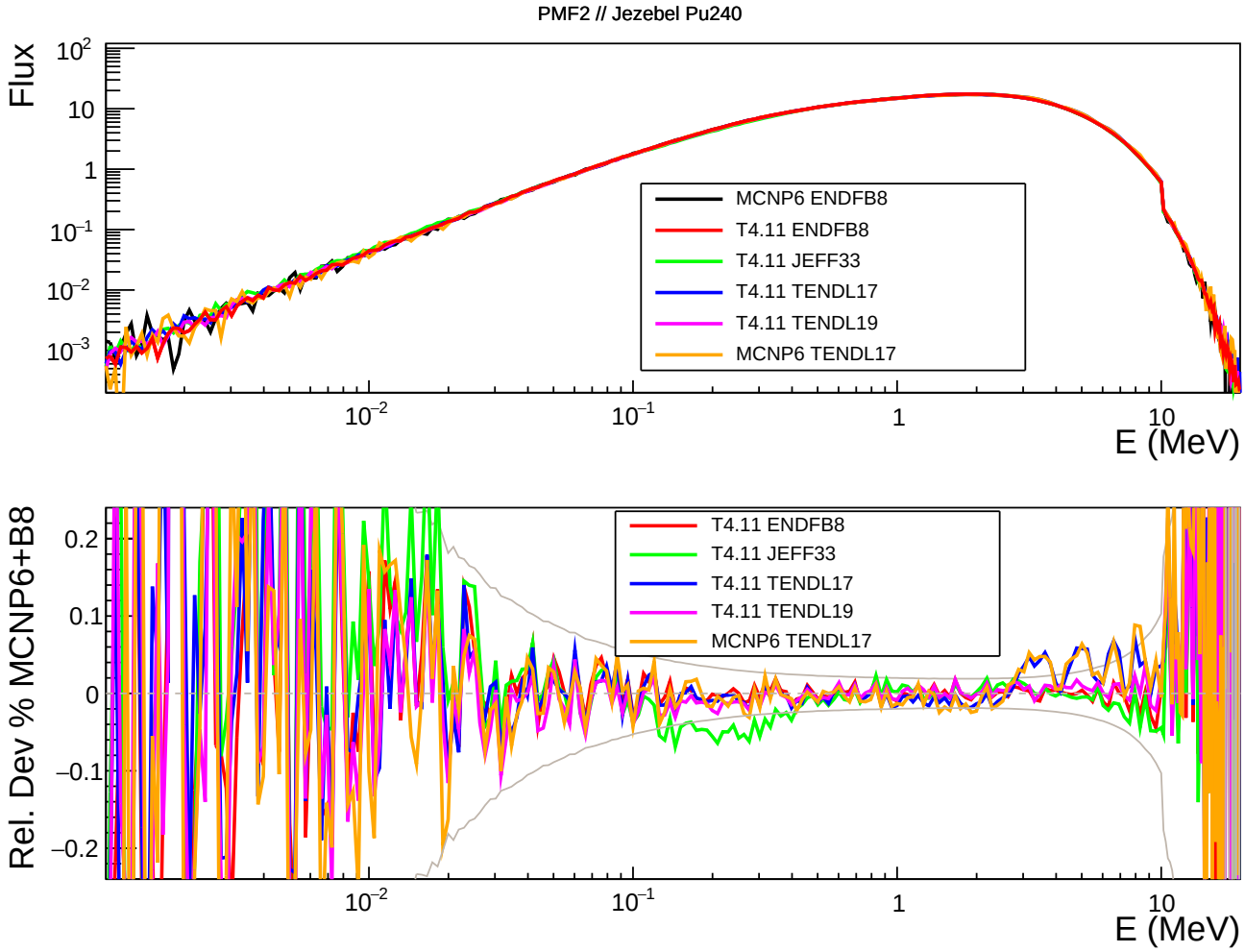

Figure 2: Results on neutron flux for PMF2 benchmark Jezebel-Pu40 in the inner sphere. Upper part : neutron flux. Lower part : ratio to MCNP5.1.40 + TENDL-19.

Code-Lib	MCNP6-B8	T4.11-B8	MCNP6-T17	T4.11-T17	T4.11-T19	T4.11-J33
k_{eff}	1.00144 (1)	1.00137 (1)	1.00507 (3)	1.00499 (1)	1.00407 (1)	1.00122 (1)

Table 3: PMF2 benchmark Jezebel-Pu240 : MCNP6 and TRIPOLI-4.11 k_{eff} calculations using ENDF/B-VIII, JEFF-3.3,TENDL-17 and TENDL-19 libraries

Reaction	MCNP6-B8	T4.11-B8	MCNP6-T17	T4-T17	T4-T19	T4-J33
U235(n,f)	9.50478E-3	9.51466E-3	9.52893E-3	9.52946E-3	9.51037E-3	9.44035E-3
U238(n,f)	1.94480E-3	1.94579E-3	1.97122E-3	1.97021E-3	1.95462E-3	1.92243E-3
Np237(n,f)	9.07541E-3	9.08266E-3	9.06010E-3	9.05747E-3	9.04452E-3	9.08843E-3

Table 4: PMF2 benchmark Jezebel-Pu40 : MCNP6, MCNP5.1.40 and TRIPOLI-4.11 reaction rates calculations using ENDF/B-VIII, JEFF-3.3,TENDL-17 and TENDL-19 libraries

2.3 HMF1

This benchmark, named Godiva, consists of a 8.7407cm enriched uranium sphere. Figure 3, Table 5 and Table 6 present results obtained with MCNP6 and and TRIPOLI-4.11 using various libraries.

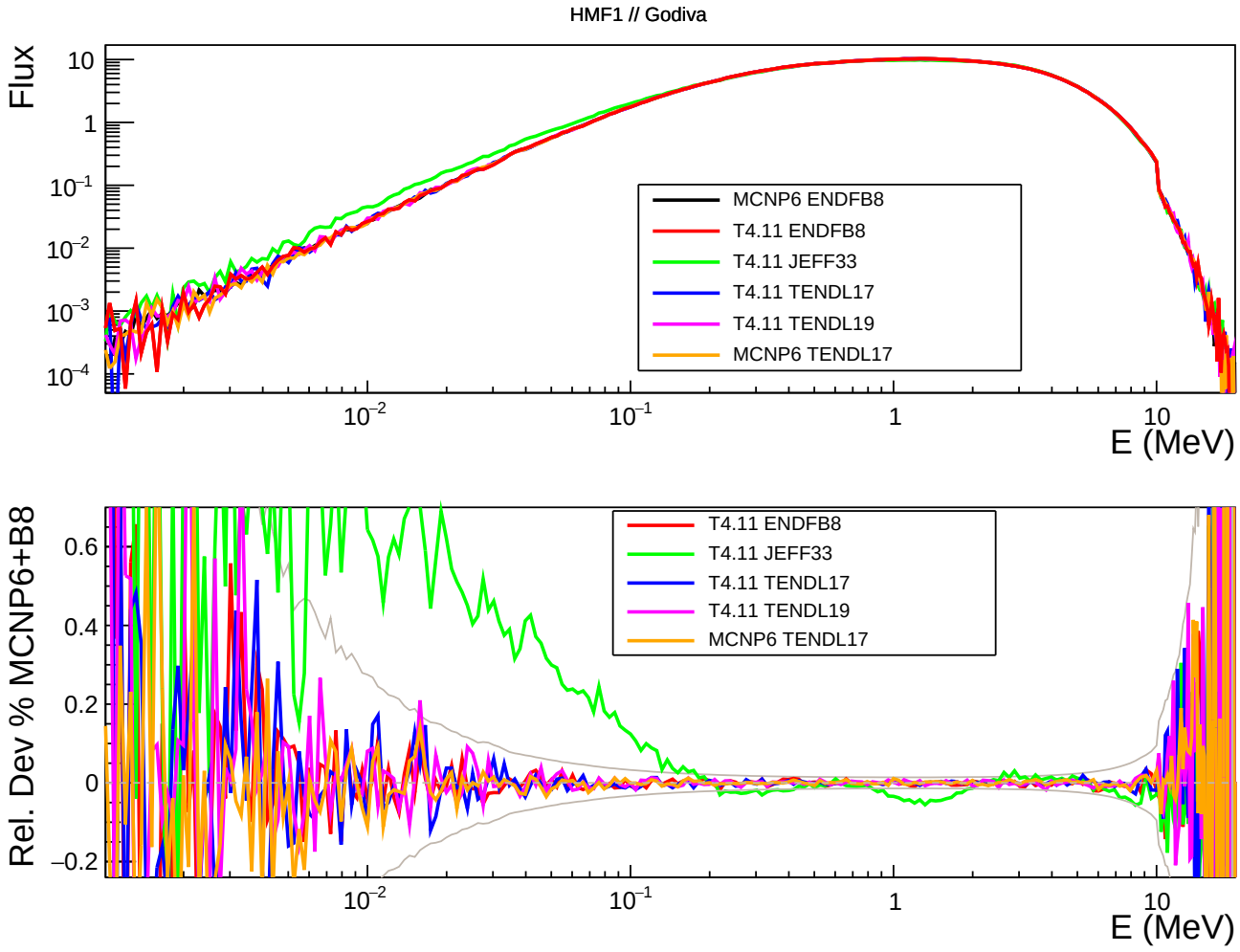

Figure 3: Results on neutron flux for HMF1 benchmark Godiva. Upper part : neutron flux. Lower part : ratio to MCNP5.1.40 + TENDL-19.

Code-Lib	MCNP6-B8	T4.11-B8	MCNP6-T17	T4.11-T17	T4.11-T19	T4.11-J33
k_{eff}	1.00005 (1)	1.00005 (2)	1.00007 (1)	1.00006 (2)	1.00004 (2)	1.00000 (2)

Table 5: HMF1 benchmark Godiva : MCNP6 and TRIPOLI-4.11 k_{eff} calculations using ENDF/B-VIII, JEFF-3.3,TENDL-17 and TENDL-19 libraries

Reaction	MCNP6-B8	T4.11-B8	T4-T17	T4.11-T17	T4.11-T19	T4.11-J33
U233(n,f)	9.99476E-3	9.99128E-3	1.00126E-2	9.99299E-3	9.99645E-3	9.95108E-3
U235(n,f)	6.33062E-3	6.32650E-3	6.34025E-3	6.32786E-3	6.33038E-3	6.35329E-3
U238(n,f)	1.00533E-3	1.00120E-3	1.00551E-3	1.00266E-3	1.00176E-3	9.84443E-4
U238(n,2n)	5.05399E-5	5.01143E-5	5.05169E-5	5.02297E-5	5.04750E-5	4.80933E-5
U238(n,γ)	4.70305E-4	4.70400E-4	4.70929E-4	4.70384E-4	4.70906E-4	4.65814E-4
Np237(n,f)	5.26386E-3	5.25636E-3	5.24478E-3	5.23231E-3	5.23179E-3	5.19058E-3
Pu239(n,f)	8.76305E-3	8.75845E-3	8.78021E-3	8.76155E-3	8.76322E-3	8.77994E-3
Al27(n,p)	1.23436E-5	1.22606E-5	1.25153E-5	1.24715E-5	1.26841E-5	1.21832E-5
Al27(n,α)	2.39645E-6	2.39239E-6	2.35992E-6	2.36234E-6	2.29219E-6	2.30904E-6
P31(n,p)	1.03396E-4	1.02696E-4	1.08184E-4	1.08092E-4	1.08869E-4	8.69660E-5
V51(n,γ)	1.74123E-5	1.74812E-5	2.07496E-5	2.06960E-5	1.87448E-5	1.89967E-5
Mn55(n,γ)	2.17244E-5	2.17022E-5	2.17299E-5	2.16727E-5	2.17059E-5	2.30888E-5
Fe55(n,p)	3.58001E-6	1.74549E-4	3.58479E-6	1.74913E-4	1.74680E-4	1.74117E-4
Co59(n,γ)	3.24904E-5	3.25108E-5	3.59061E-5	3.58074E-5	3.49608E-5	3.59321E-5
Cu63(n,2n)	2.51750E-7	3.21107E-7	3.26738E-7	3.25373E-7	3.19994E-7	3.24059E-7
Cu63(n,γ)	7.49523E-5	7.53247E-5	6.62568E-5	6.57240E-5	6.77657E-5	7.85098E-5
Cu65(n,γ)	4.14195E-5	4.15509E-5	3.41071E-5	3.43542E-5	3.88907E-5	4.84814E-5
As75(n,γ)	2.78627E-4	2.79389E-4	2.50062E-4	2.50355E-4	2.77302E-4	2.96955E-4
Br79(n,γ)	4.56530E-4	4.56015E-4	4.09332E-4	4.10330E-4	4.07188E-4	4.38631E-4
Br81(n,γ)	1.81168E-4	1.81057E-4	1.77283E-4	1.76953E-4	1.75809E-4	1.85991E-4
Rb85(n,γ)	2.12790E-4	2.13377E-4	1.59030E-4	1.58719E-4	1.52136E-4	1.65535E-4
Rb87(n,γ)	2.29133E-5	2.23916E-5	1.73878E-5	1.73980E-5	1.63970E-5	1.78907E-5
Y89(n,γ)	3.25584E-5	3.29053E-5	3.05032E-5	3.04500E-5	2.36347E-5	3.27710E-5
Nb93(n,γ)	2.16873E-4	2.14814E-4	2.04907E-4	2.04486E-4	2.01799E-4	2.26404E-4
Rh103(n,γ)	6.37924E-4	6.37973E-4	7.40516E-4	7.40185E-4	7.32722E-4	7.39772E-4
Ag107(n,γ)	8.04753E-4	8.03234E-4	6.48723E-4	6.48725E-4	5.02904E-4	5.37838E-4
In115(n,γ)	1.05078E-3	1.05061E-3	9.66154E-4	9.64999E-4	1.50437E-3	1.11990E-3
Sb121(n,γ)	6.62614E-4	6.62933E-4	6.02459E-4	6.01712E-4	5.22740E-4	5.42557E-4
I127(n,γ)	5.69463E-4	5.69859E-4	4.74874E-4	4.75438E-4	4.69453E-4	5.77929E-4
La139(n,γ)	4.26933E-5	4.26586E-5	4.13673E-5	4.14678E-5	4.03231E-5	4.38689E-5
Ta181(n,γ)	7.62225E-4	7.62726E-4	6.47056E-4	6.46779E-4	6.47793E-4	6.74115E-4
Re185(n,γ)	1.29660E-3	1.29715E-3	1.67415E-3	1.67176E-3	1.65087E-3	1.73575E-3
Re187(n,γ)	9.75213E-4	9.74979E-4	9.32344E-4	9.32033E-4	9.28151E-4	9.89023E-4
Ir193(n,γ)	8.98508E-4	8.98692E-4	7.23846E-4	7.22762E-4	7.42533E-4	9.41246E-4
Au197(n,γ)	5.98694E-4	5.98624E-4	6.00864E-4	6.00689E-4	5.96678E-4	6.19437E-4
Tl205(n,γ)	4.63285E-5	4.60939E-5	6.28827E-5	6.40446E-5	6.58028E-5	8.25990E-5
Bi209(n,γ)	1.45380E-5	1.45349E-5	1.16785E-5	1.16671E-5	1.16152E-5	1.01048E-5

Table 6: HMF1 benchmark Godiva : MCNP6 and TRIPOLI-4.11 reaction rates calculations using ENDF/B-VIII, JEFF-3.3,TENDL-17 and TENDL-19 libraries

2.4 IMF7

The modelling of the geometry used for comparisons of fluxes and reaction rates is the one considered in the CONDERC/MCNP6 document. Figure 4, Table 7 and Table 8 present results obtained with MCNP6 and TRIPOLI-4.11 using various libraries.

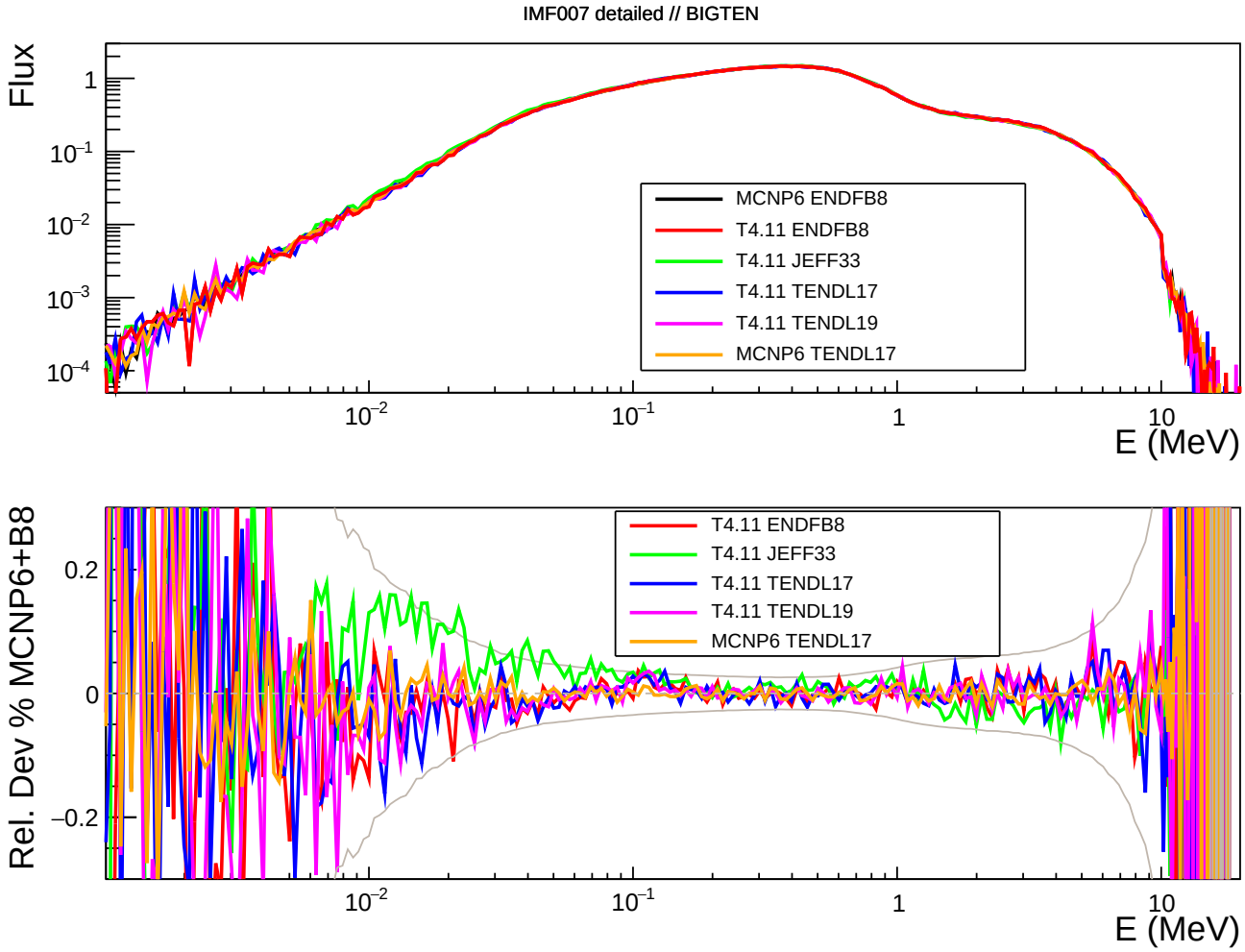

Figure 4: Results on neutron flux for IMF7-2Z benchmark BigTen-2Z. Upper part : neutron flux. Lower part : ratio to MCNP5.1.40 + TENDL-19.

Code-Lib	MCNP6-B8	T4.11-B8	MCNP6-T17	T4.11-T17	T4.11-T19	T4.11-J33
k_{eff}	1.00427 (1)	1.00490 (2)	1.00429 (1)	1.00489 (2)	1.00484 (2)	1.00527 (1)

Table 7: IMF7 benchmark Bigten : MCNP6 and TRIPOLI-4.11 k_{eff} calculations using ENDF/B-VIII, JEFF-3.3,TENDL-17 and TENDL-19 libraries

Reaction	MCNP6-B8	T4.11-B8	MCNP6-T17	T4.11-T17	T4.11-T19	T4.11-J33
U235(n,f)	8.98489E-4	8.98127E-4	8.98264E-4	8.98360E-4	8.98731E-4	9.13897E-4
U235(n,f)	1.39369E-3	1.39329E-3	1.39325E-3	1.39363E-3	1.39393E-3	1.41588E-3
U238(n,f)	3.20693E-5	3.21240E-5	3.20547E-5	3.21689E-5	3.20950E-5	3.07152E-5
U238(n,2n)	1.50256E-6	1.48308E-6	1.48605E-6	1.51082E-6	1.50661E-6	1.39288E-6
U238(n,γ)	9.45863E-5	9.42148E-5	9.45365E-5	9.42690E-5	9.43096E-5	9.27498E-5
Np237(n,f)	2.81956E-4	2.81946E-4	2.81429E-4	2.81652E-4	2.81494E-4	2.80864E-4
Pu239(n,f)	1.05124E-3	1.05119E-3	1.05081E-3	1.05150E-3	1.05156E-3	1.07208E-3
Sc45(n,γ)	1.31128E-5	1.30791E-5	1.20739E-5	1.20181E-5	1.28762E-5	1.25625E-5
Mn55(n,γ)	5.84896E-6	5.75160E-6	5.84280E-6	5.81838E-6	5.82686E-6	6.09567E-6
Fe58(n,γ)	4.51291E-6	4.52947E-6	3.26447E-6	3.25737E-6	3.29346E-6	3.95945E-6
Co59(n,γ)	7.59808E-6	7.56676E-6	8.79323E-6	8.62140E-6	8.17943E-6	8.95645E-6
Cu63(n,γ)	1.59456E-5	1.60518E-5	1.42873E-5	1.42099E-5	1.53111E-5	1.71177E-5
Y89(n,2n)	1.44837E-8	1.41702E-8	1.95530E-8	1.69550E-8	1.72253E-8	1.50139E-8
Y89(n,γ)	6.11889E-6	6.08737E-6	5.98416E-6	5.94330E-6	3.20614E-6	6.27702E-6
In113(n,γ)	2.54436E-4	2.53702E-4	1.85576E-4	1.85168E-4	2.36162E-4	1.90541E-4
In115(n,γ)	2.08590E-4	2.08010E-4	1.92291E-4	1.91854E-4	2.74722E-4	2.17392E-4
Eu151(n,γ)	7.69320E-4	7.66724E-4	8.65700E-4	8.64336E-4	8.93607E-4	9.43436E-4
Eu153(n,γ)	5.38536E-4	5.36937E-4	4.99363E-4	4.98630E-4	4.86146E-4	5.39088E-4
Tm169(n,2n)	3.67530E-7	3.67215E-7	3.87226E-7	3.80817E-7	3.80318E-7	3.35392E-7
Tm169(n,γ)	2.28759E-4	2.28233E-4	2.14963E-4	2.14448E-4	2.11829E-4	2.25958E-4
Lu176(n,γ)	4.20052E-4	4.19385E-4	4.39328E-4	4.38659E-4	4.35443E-4	4.58402E-4
Ta181(n,γ)	1.78627E-4	1.78044E-4	1.64123E-4	1.63688E-4	1.64097E-4	1.68154E-4
W180(n,γ)	1.64998E-4	1.64835E-4	1.54042E-4	1.53886E-4	1.22059E-4	1.35832E-4
W184(n,γ)	6.53814E-5	6.52632E-5	6.25397E-5	6.25557E-5	6.27552E-5	5.41949E-5
W186(n,γ)	4.72464E-5	4.71866E-5	4.82826E-5	4.82178E-5	4.80999E-5	6.47782E-5
Ir191(n,2n)	3.69868E-7	3.69318E-7	4.55240E-7	4.48829E-7	4.24511E-7	3.47530E-7
Ir191(n,γ)	2.93079E-4	2.92234E-4	3.30456E-4	3.30299E-4	3.29341E-4	3.10236E-4
Ir193(n,γ)	2.39969E-4	2.39240E-4	2.04620E-4	2.04472E-4	2.06085E-4	2.51154E-4
Au197(n,2n)	3.03828E-7	3.02915E-7	3.38191E-7	3.31110E-7	3.11146E-7	2.86005E-7
Au197(n,γ)	1.48642E-4	1.48421E-4	1.50573E-4	1.50460E-4	1.48374E-4	1.52683E-4
Am241(n,γ)	6.82781E-4	6.81952E-4	7.15054E-4	7.14752E-4	7.15295E-4	7.27543E-4
Li6(n,t)	5.88273E-4	5.87743E-4	5.87956E-4	5.87979E-4	5.88148E-4	5.98326E-4
B10(n,α)	8.40897E-4	8.39418E-4	8.40812E-4	8.39934E-4	8.40455E-4	8.75857E-4
Al27(n,p)	3.78495E-7	3.78702E-7	3.83409E-7	3.86261E-7	3.92823E-7	3.66611E-7
Al27(n,α)	7.12392E-8	7.05928E-8	7.01437E-8	7.06534E-8	6.83632E-8	6.66829E-8
Ti46(n,p)	1.01577E-6	1.01586E-6	1.10908E-6	1.11782E-6	1.11569E-6	1.06965E-6
Ti47(n,p)	1.90098E-6	1.90380E-6	1.76937E-6	1.77851E-6	1.77481E-6	1.71954E-6
Ti48(n,p)	3.49472E-8	3.46672E-8	2.99957E-8	3.01590E-8	3.01261E-8	2.80572E-8
Fe54(n,p)	7.50550E-6	7.52091E-6	7.51928E-6	7.56209E-6	7.54955E-6	6.60433E-6
Fe56(n,p)	1.07519E-7	1.06709E-7	1.07844E-7	1.08734E-7	1.08546E-7	1.00186E-7
Co59(n,2n)	1.92429E-8	1.89330E-8	2.34782E-8	2.12074E-8	2.16279E-8	1.86502E-8
Co59(n,p)	1.38816E-7	1.37841E-7	1.37768E-7	1.38720E-7	1.38593E-7	1.32147E-7
Ni58(n,p)	1.03569E-5	1.02752E-5	1.03754E-5	1.04325E-5	1.04132E-5	1.01438E-5

Table 8: IMF7-detailed benchmark : MCNP6 and TRIPOLI-4.11 reaction rates calculations using ENDF/B-VIII, JEFF-3.3,TENDL-17 and TENDL-19 libraries

3 Conclusion on criticality benchmarks

We can make several remarks on these criticality cases:

- We observe a very good agreement on the keff between MCNP6 and TRIPOLI-4. For these four benchmarks, we systematically have MCNP6 results with the ENDF/B-VIII and TENDL-17 libraries. The agreements with the TRIPOLI-4 results are excellent. The reaction rates are also very close for the dosimeters calculated with the two codes using the same libraires. There is one exception to this last remark, the Fe56(n,p) reaction for Godiva bencmark (HMF1).

- The JEFF-3.3 library gives quite different keffs, in any case not statistically compatible for the two Jezebel benchmarks with plutonium (PMF1 and PMF2) and for the Bigten benchmark (IMF7).For the Godiva benchmark, the agreement on the two codes is very good.

- Comparison of the neutron fluxes calculated in the small spheres at the centres of the configurations reveals discrepancies between the libraries, while the calculation of the multiplier coefficient is in agreement. This is particularly the case for Godiva, where the fluxes calculated by TRIPOLI-4 are very different between the JEFF-3.3 library and the others, while the keff is in excellent agreement.

- The probability tables of NJOY/PURR and CALENDF do not take into account the same cross sections. Indeed, for NJOY/PURR, the probability tables concern the total cross-section, elastic scattering, radiative capture and induced fission. CALENDF calculates probability tables for the competitive cross section, which is the inelastic scattering towards the first excited state for U238. This leads to an impact of the order of 50-60 pcm for the IMF-7 benchmark [12].

4 Iron evaluation files

Iron isotopes are very important for the structural materials used, for example, in reactors. They are exposed to high energy neutron fluxes which can damage their structures. The study of neutron propagation in these types of materials is particularly important. We have selected a benchmark to test these evaluations: ASPIS.

4.1 ASPIS benchmark

The goal of this experiment is to test nuclear data and calculation methods on a configuration close to those of light water reactors. This experimental device is installed on the NESTOR reactor at Winfrith. A fission source is driven by thermal neutrons leaking from the outer graphite reflector of NESTOR. This benchmark was realised to study the propagation of neutrons in an iron bulk. The main nucleus in the composition structure is 56Fe whose evaluation

is done using linear-linear interpolation in energy-angle distributions (in particular for continuous inelastic scattering with a threshold at 4.5 MeV). Three high energy dosimetric responses are measured at different depths of penetration in the iron bulk (from 5.5 to 114 cm) :

- 103Rh(n,n') reaction with an energy threshold of 40keV
- 115In(n,n') reaction with an energy threshold of 339keV
- 32S(n,p)32P reaction with an energy threshold of 1.6MeV

The cumulative systematic and statistic errors for the dosimeters are respectively : 14% for 103Rh, 7:5% for 115In and 10% for 32S.

4.2 TRIPOLI-4 calculations using various libraries

The figure shows the neutron propagation results in the iron bulj as a C/E ratio for the three dosimeters mentioned. The calculations are performed with TRIPOLI-4 and several recent libraries.
Two libraries give quite similar results and relatively good agreement on the experimental measurements: ENDF/B-VII.1 and JENDL-4.0. We will use JENDL-4.0 as a reference library for two complementary studies.
The TENDL-19 library shows a clear deficit in the neutron flux as the neutrons propagate through the iron bulk, whatever the dosimeter considered (range of a few hundred keV or a few MeV)

We were looking at the comparison between TENDL-19 and JENDL-4.0. For this purpose, we took the JENDL-4.0 evaluation for Fe56 as a reference and we overwritten some data from the file with data from TENDL-19. The following two subsections present the results obtained with these different evaluations of Fe56 according to the modifications applied.

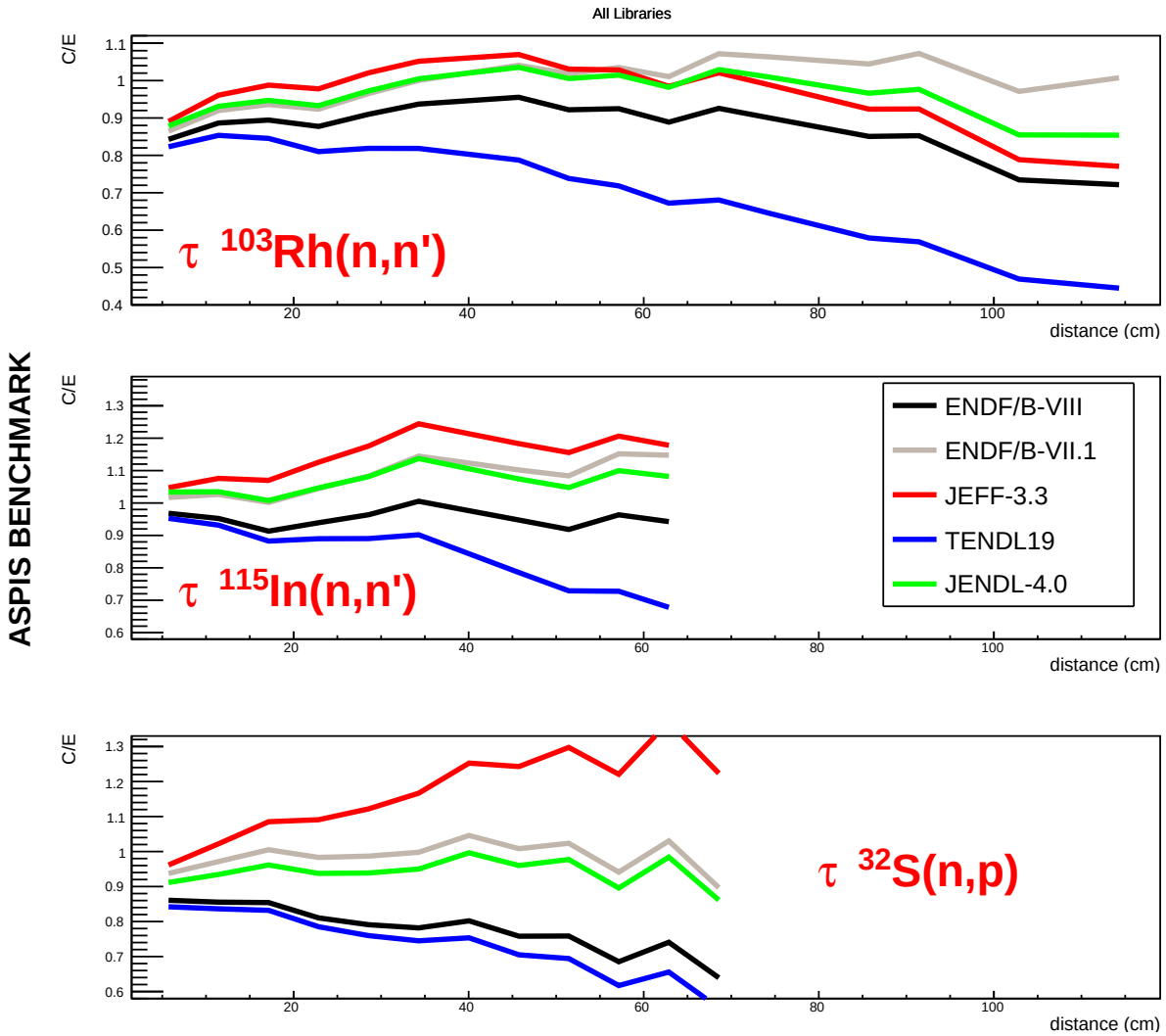

Figure 5: ASPIS benchmarks: C/E TRIPOLI-4 results for three dosimeters using various libraries.

4.2.1 Impact of scattering cross sections

Elastic and inelastic scattering cross sections naturally play an important role in neutron propagation. The impact of a modification on the inelastic cross sections is very important because the kinetic energy of the neutron at the exit of inelastic scattering is much more modified than for elastic scattering.
For the following comparison, all nuclei, except Fe56, are systematically from JENDL-4.0. Figure 6 shows the results of the TRIPOLI-4 simulations on the ASPIS benchmark, indicating the relative difference to the results obtained with the full JENDL-40 library (including Fe56). Four calculations are compared:

- The black curves show the calculations with the Fe56 nucleus from the TENDL19 library
- The red curves show the calculations performed with a JENDL-4.0 file for Fe56 in which the cross sections (MF3) and anisotropies (MF4) of the discrete elastic and inelastic scatterings have been replaced by those of TENDL19.
- The blue curves are obtained with the modified red curve files but the continuous inelastic scattering data is also modified and added from TENDL19
- The green curves correspond to the previous evaluation but the scattering radius (AP) for L=1 in the RRR is modified to take the value of that from TENDL19

We thus observe that for the lowest energy dosimeters (Rh103 and In115), it is the difference in the scattering radius between the JENDL40 file and the TENDL file that explains the differences between TENDL19 and JENDL40. On the other hand, at higher energies (dosimeter S32), the impact of continuous inelastic scattering is very important. There is an obvious compensation between discrete scattering and continuous inelastic scattering (MT91)

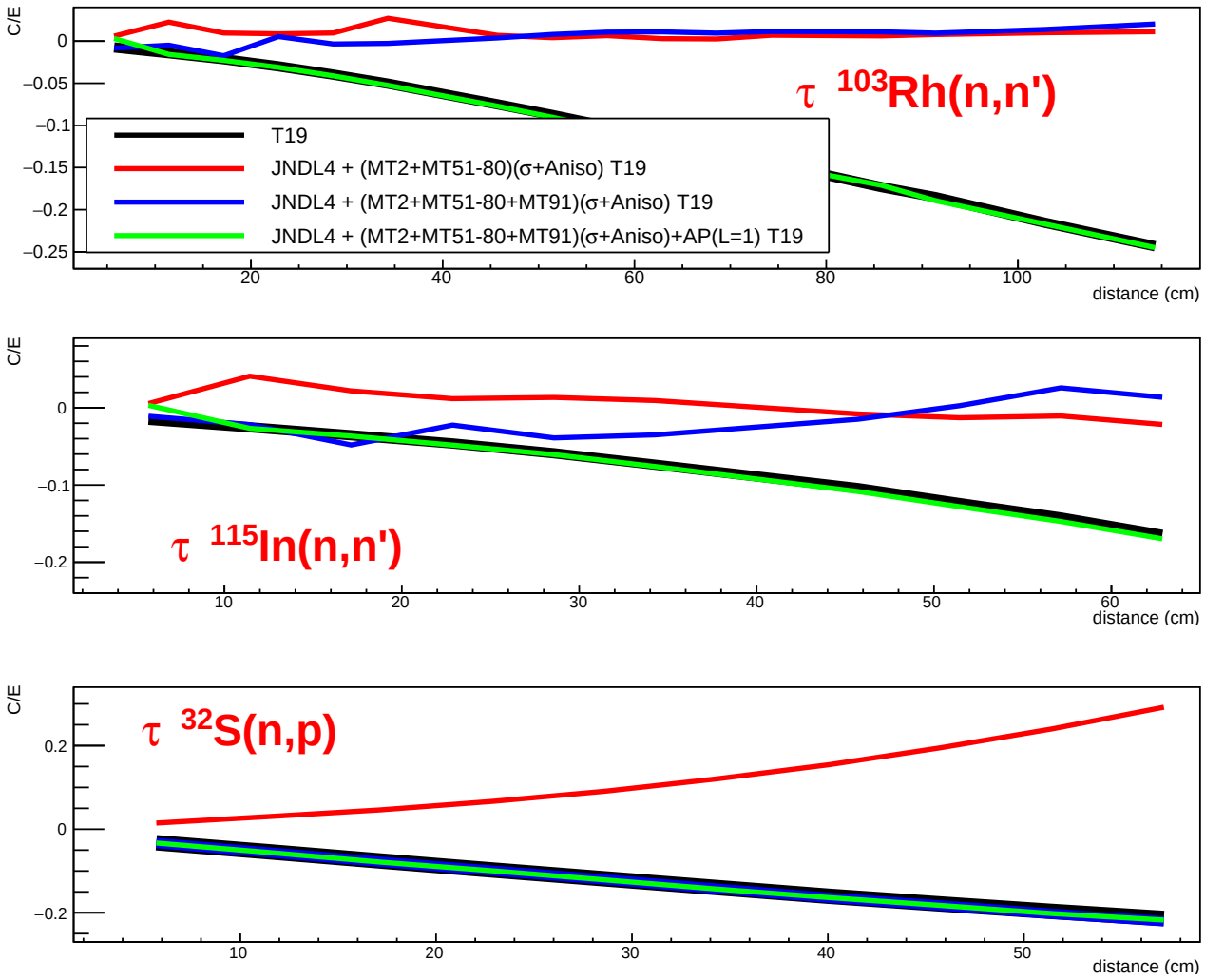

Figure 6: ASPIS benchmarks: impact of scattering cross sections.

4.2.2 Impact of scattering angular distributions

In this subsection, we wish to highlight the impact of scattering anisotropies, in particular, for elastic scattering. For the following calculations, all nuclei evaluations, except for Fe56, are taken from JENDL-4.0. The results presented are calculation/calculation ratios compared to the results obtained with the full JENDL-4.0 library. Figure 7 presents results on ASPIS benchmark for these calculations :

- black results : The evaluation of Fe56 is from ENDF/B-VIII
- red results: The evaluation of Fe56 is that of JENDL-4.0, but we have replaced the elastic scattering cross-section by that of ENDF/B-VIII.
- green results: We have taken the previous file (red curve) and replaced the elastic scattering anisotropy by that of ENDF/B-VIII
- blue results: In the previous evaluation (green curve), we have replaced the effective cross-section and the anisotropy for the inelastic scattering towards the first excited state (MT51)

The differences between the red and green curves show the impact of the anisotropy of the elastic scattering. We observe that taking into account the data for inelastic scattering towards the first excited state partly compensates for this impact (differences between green and blue curves).

5 Conclusions on ASPIS-iron benchmark

The cross sections are particularly important for this ASPIS benchmark, which simulates neutron transport through a large thickness of steel. For shielding benchmark, in particular for the configuration studied in this document, both inelastic and elastic scatterings are important, in term of cross sections, but that their angular distribution also are, that compensation effect seems to be at play there. A further study on these aspects for structural materials (iron, nickel, chrome, steel components) would be very interesting. Comparisons for higher energy neutron fluxes could be made.

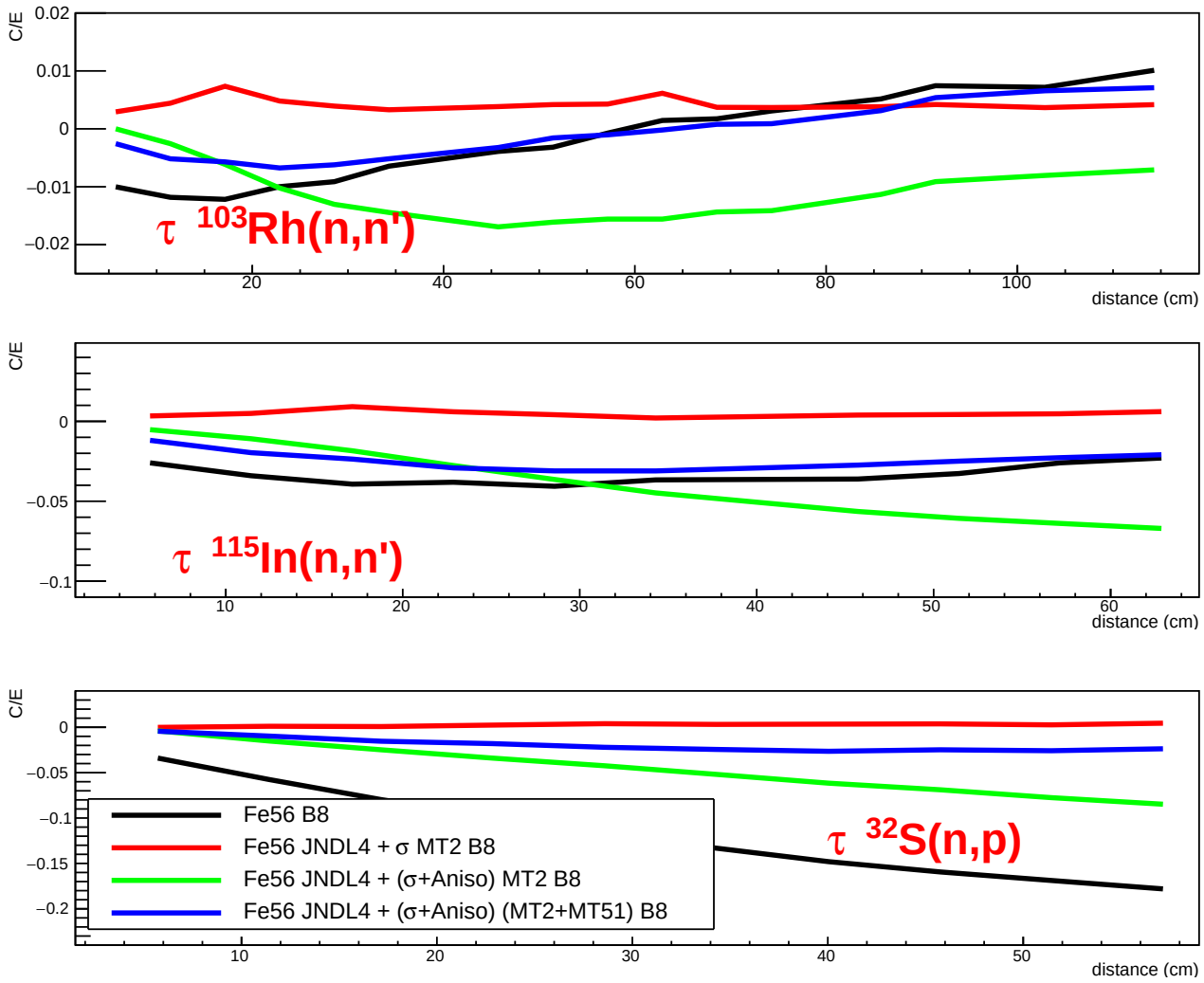

Figure 7: ASPIS benchmarks: impact of scattering angular distributions.

References

[1] KONING, A. J., ROCHMAN, D., SUBLET, J.-Ch, et al. "TENDL: complete nuclear data library for innovative nuclear science and technology". Nuclear Data Sheets, 2019, **155**, p. 1-55.

[2] Plompen, A. J. M., & al. *The joint evaluated fission and fusion nuclear data library, JEFF-3.3.*, The European Physical Journal A, 2020, **56.7**, 1-108.

[3] Shibata, K. & al. *JENDL-4.0 : A new library for nuclear science and Engineering*, J. Nucl. Sci. Technol., 2011, **48 (1)**, 1-30

[4] BROWN, David A., CHADWICK, M. B., CAPOTE, R., et al. "ENDF/B-VIII. 0: the 8th major release of the nuclear reaction data library with CIELO-project cross sections, new standards and thermal scattering data". Nuclear Data Sheets, 2018, **148**, p. 1-142.

[5] BRUN, E. et al., "Tripoli-4®, CEA, EDF and AREVA reference Monte Carlo code", Annals of Nuclear Energy **82**, 151-160 (2015).

[6] MCNP 5.1.40 RSICC Release Notes, Los Alamos Report, LA-UR-05-8617, (2005).

[7] KAHLER III, A. C. and MACFARLANE, R. NJOY2016. Los Alamos National Lab. (LANL), Los Alamos, NM (United States), 2016. LA-UR-17_20093 (2017).

[8] SUBLET, J.-Ch, RIBON, P., and COSTE-DELCLAUX, M. "CALENDF-2010: user manual". 2011. CEA-R-6277 (2011).

[9] CHADWICK, M. B., HERMAN, M., OBLOŽINSKÝ, P., et al. "ENDF/B-VII. 1 nuclear data for science and technology: cross sections, covariances, fission product yields and decay data". Nuclear data sheets, 2011, **112**, no 12, p. 2887-2996.

[10] BRIGGS, J., et al. "International handbook of evaluated criticality safety benchmark experiments". Nuclear Energy Agency, NEA/NSC/DOC (95), 2004, **3**, p. l.

[11] MCLANE, V. "ENDF-102 data formats and procedures for the evaluated nuclear data file ENDF-6". Brookhaven National Lab., 2001.

[12] MACFARLANE, R., BLOMQUIST, R., CULLEN, D. and SUBLET J.-C. "A code comparison study for the Bigten critical assembly", LA-UR-08-4668.